

Published in final edited form as:

Nature. 2012 November 22; 491(7425): 594–598. doi:10.1038/nature11673.

Aberrant light directly impairs mood and learning through melanopsin-expressing neurons

Tara LeGates^{1,*}, Cara Altimus^{1,*}, Hui Wang², Hey-Kyoung Lee², Sunggu Yang², Haiqing Zhao¹, Alfredo Kirkwood², Todd Weber^{3,#}, and Samer Hattar^{1,2,#}

¹Department of Biology, Johns Hopkins University, Baltimore, MD 21218, USA

²Department of Neuroscience, Johns Hopkins University, Baltimore, MD 21218, USA

³Department of Biology, Rider University, Lawrenceville, NJ 08648, USA

Keywords

ipRGCs; Circadian; Sleep; Jet-lag; Seasonal affective disorder; Shift-work; Anxiety; and Depression

The daily solar cycle allows organisms to synchronize their circadian rhythms and sleep wake cycles to the correct temporal niche¹. Changes in day length, shift-work, and transmeridian travel lead to mood alterations and cognitive function deficits². Sleep deprivation and circadian disruption underlie mood and cognitive disorders associated with irregular light schedules². Whether irregular light schedules directly affect mood and cognitive functions in the context of normal sleep and circadian rhythms remains unclear. Using an aberrant light cycle that neither changes the amount and architecture of sleep nor causes changes in the circadian timing system, we show that light directly regulates mood-related behaviors and cognitive functions in mice. Animals exposed to the aberrant light cycle maintain daily corticosterone rhythms, but the overall levels of corticosterone are increased. Despite normal circadian and sleep structures, these animals show increased depression-like behaviors and impaired hippocampal long-term potentiation and learning. Administration of antidepressant drugs, fluoxetine or desipramine, restores learning in mice exposed to the aberrant light cycle, suggesting that the mood deficit precedes the learning impairments. To determine the retinal circuits underlying this impairment of mood and learning, we examined the behavioral consequences of this light cycle in animals that lack intrinsically photosensitive retinal ganglion cells (ipRGCs). In these animals, the aberrant light cycle does not impair mood and learning, despite the presence of the majority of conventional retinal ganglion cells and the ability of these animals to detect light for image formation. These findings demonstrate the ability of light to directly influence cognitive and mood functions through ipRGCs.

*Correspondence to Samer Hattar (shattar@jhu.edu) and Todd Weber (tweber@rider.edu). Editorial correspondence: Dr. Samer Hattar, Associate Professor, Johns Hopkins University, Department of Biology, 3400 N. Charles Street/Mudd 227, Baltimore, MD 21218, Tel: 410-516-4231, fax: 410-516-5213, shattar@jhu.edu.

#These two authors contributed equally to the work.

Author Contributions

T.A.L., C.M.A., H.Z., E.T.W., and S.H. designed experiments. T.A.L. and C.M.A. carried out experiments. H.W., H-K.L., S.Y., and A.K. designed and performed electrophysiological experiments. T.A.L., C.M.A., H.Z., E.T.W., and S.H. wrote the paper.

Reprints and permissions information is available at www.nature.com/reprints

The authors declare no competing financial interests.

In mammals, all light information for image formation and regulation of behavior is detected by the retina and signaled to relevant brain targets through retinal ganglion cells (RGCs). The majority of RGCs signal light to thalamic relay nuclei and then to the visual cortex for image functions. A population of intrinsically photosensitive RGCs (ipRGCs^{3,4}), which predominantly signal light information for non-image forming visual functions expresses the photopigment melanopsin and can be distinguished from the majority of RGCs that support image tracking and detection⁵. ipRGCs project to several hypothalamic and preoptic areas such as the suprachiasmatic nucleus (SCN), subparaventricular nucleus (SPZ), and ventrolateral preoptic area (VLPO) to regulate circadian rhythms and sleep. However, they also project to limbic regions such as the lateral habenula and the medial amygdala^{4,6}, highlighting a possible role in the regulation of cognitive functions.

To determine how aberrant light influences behavior, we subjected mice to an ultradian cycle consisting of 3.5-hour light and 3.5-hour dark (T7). Our previous studies showed that this T7 aberrant light cycle does not affect the architecture (Figure S1) or total sleep levels when compared to 12:12 light-dark (T24) control cycle⁹. We also determined whether the circadian timing system was disrupted in the T7 animals by measuring core body temperature and general activity rhythms. The T7 cycle does not cause circadian arrhythmicity in either output rhythm (Figure 1A–B and S2), although the circadian period is lengthened.

To determine if the T7 cycle influences the molecular basis of the circadian clock, we measured circadian changes of a molecular clock component (Period2) in central (SCN) and peripheral (liver) tissues. Mice housed in the T7 cycle show similar rhythms and localization of PER2 expression in the SCN as compared to littermates housed in the T24 cycle (Figure 1C and S3), indicating no disruption of internal rhythmicity of the SCN pacemaker. Furthermore, *Per2* levels in the liver from mice housed in the T24 or T7 light cycle were intact and showed similar phases (Figure 1D). Together, these data show that the T7 light cycle does not disrupt sleep or cause circadian arrhythmicity. Although the circadian timing system and sleep remain intact under the T7 light cycle, mice are exposed to light pulses at all circadian phases during the experimental time course due to the mismatch between the imposed light cycle and the period length. Thus, the T7 cycle will allow us to determine the direct influence of aberrant light exposure on mood and cognitive functions.

The T7 paradigm causes light to appear during the night (active) phase of the animals' cycle. To determine which brain regions respond to light presented at night, we measured c-fos expression in response to an acute light pulse. Upon examination of ipRGC targets that are part of or known to influence the limbic system, we found light-induced c-fos expression in the amygdala, lateral habenula, and SPZ (Figure S4). This suggests that light input particularly when presented at an aberrant time of day may influence regions of the brain involved in mood and cognitive functions.

Shorter daylength during the winter months leads to a seasonal form of depression known as seasonal affective disorder (SAD), and appropriately timed light therapy can alleviate the symptoms of SAD¹⁰. We, thus, investigated whether the T7 cycle, which exposes animals to light at inappropriate times, causes depression-like behaviors in mice by evaluating sucrose anhedonia and behavioral despair in the forced swim test (FST). Mice housed in the T7 cycle showed decreased sucrose preference indicating an increase in depression-like behavior (Figure 1E and S5). This was further supported by the FST; mice housed in the T7 cycle spent significantly more time immobile as compared to mice housed in the T24 cycle (Figure 1F).

An established association with depression is increased serum corticosterone levels¹¹. We measured serum corticosterone in animals housed in T24 or T7 cycles at four time points across the day. While we found an intact circadian rhythm in corticosterone with a phase similar to mice housed in the T24 cycle, the overall levels of corticosterone were increased in mice housed in the T7 light cycle (Figure 1G).

Increases in corticosterone levels as well as anhedonia are correlated with increased stress and anxiety¹². To assay anxiety-like behavior, we used three tests: open field test, light-dark box, and elevated plus maze. We found no significant difference between animals maintained in the T24 cycle and those in the T7 cycle (Figure S6). These results show that the T7 cycle does not globally influence behavior but specifically elicits depression-and not anxiety-like behaviors.

Increased serum corticosterone levels and depression have been closely associated with hippocampal learning deficits¹³. We conducted a hippocampal-dependent task, the Morris Water Maze (MWM) (Figure 2A–D). In the MWM, the T7 mice required significantly more trials to achieve the same latency in locating a hidden platform compared to T24 mice (Figure 2B), despite similar swim speeds. All our measurements were done during the day in the T24 mice (Figure S7). Previous studies using the MWM have shown that mice use a hippocampal-dependent spatial strategy and a hippocampal-independent non-spatial strategy to locate the platform¹⁴. We sought to determine whether the deficit in learning acquisition in the T7 mice was due to the lack of hippocampal-dependent spatial learning. We, therefore, conducted a probe trial, in which the platform in the water maze was removed from the target quadrant (Figure 2C)¹⁵. We found that mice housed in the T24 cycle showed a significant preference for the target quadrant, whereas mice housed in the T7 cycle showed no preference for the target quadrant (Figure 2C). Using a reversal assay, mice housed in the T24 cycle required significantly more trials to locate the platform in the new quadrant, whereas the T7 mice showed no change in the latency to locate the platform (Figure 2D). This further supports the dependence of T7 mice on a non-spatial escape strategy, highlighting a hippocampal-dependent learning deficit.

Spatial learning deficits are usually associated with long-term potentiation¹⁶ (LTP) decrement in the hippocampus. We found that mice housed in both the T24 and T7 cycles have similar basal synaptic release at the Schaffer collaterals in the hippocampus (Figure 2E and F). However, mice housed in a T7 cycle showed impaired LTP in response to both 1 and 4 pulses of theta burst stimulation (Figure 2G and H). We found no difference in low frequency stimulation-induced long-term depression (LTD) between mice housed in the T24 and T7 cycles (Figure 2I). Impaired LTP with no change in LTD has been previously associated with sleep deprivation¹⁷. The selective LTP deficits observed in mice housed in the T7 aberrant light cycle independent of sleep deprivation indicates that learning impairments due to inappropriate light exposure and sleep deprivation may use similar neural pathways (see model: Figure S13).

To determine if the learning deficits in the T7 cycle extend to tasks involved in hippocampal-dependent recognition memory, we conducted the Novel Object Recognition test¹⁸. Mice housed in the T24 cycle showed a significant preference for the novel object (Figure 2J). In contrast, mice housed in the T7 cycle showed no preference for a novel object from a familiar object (Figure 2J).

To investigate whether antidepressants could rescue the learning deficits observed in T7 mice, we chronically administered fluoxetine to T24 and T7 mice (Figure 3A). Chronic fluoxetine treatment decreased depression-like behavior in mice housed in the T7 cycle (Figure 3B). Furthermore, this treatment was able to rescue the learning deficit observed in

the Novel Object Recognition test (Figure 3C). In support of this behavioral rescue of hippocampal function, chronic fluoxetine treatment also rescued the LTP deficit induced by the T7 cycle (Figure 3D). Subchronic fluoxetine treatment did not rescue the learning defect observed in mice housed in the T7 cycle (Figure S8), consistent with published reports²⁰. We also used desipramine, a tricyclic antidepressant, and found that desipramine restored learning (Figure S9 and supplementary text). These results show that the detrimental behavioral changes induced by aberrant light exposure can be alleviated with antidepressant administration.

To determine the mechanism by which fluoxetine restores learning, we measured the circadian period in T7 mice treated with fluoxetine. Although fluoxetine can phase shift the circadian oscillator²¹, chronic administration of fluoxetine did not change the circadian period in mice housed in the T7 cycle (Figure S10). We then examined the corticosterone rhythms in fluoxetine-treated T7 mice and showed that corticosterone rhythms persist with lower overall levels compared to untreated mice (Figure 3E). These data indicate that fluoxetine treatment does not alter circadian rhythms but instead lowers the level of corticosterone, which could lead to lower depression-like behavior and better learning.

Studies have suggested that ipRGCs, in addition to affecting reflexive, irradiance-dependent non-image forming visual functions, might directly influence higher cognitive functions and brain processing of emotions^{22–25}. To directly determine if ipRGCs mediate the effects of the T7 cycle on mood and learning, we tested mice lacking ipRGCs (*Opn4^{aDTA/aDTA}*, herein referred to as aDTA mice). While the majority of ipRGCs are ablated, these mice still retain more than 95% of RGCs and are capable of image formation⁵. First, we compared wild type to aDTA littermates and showed no differences in baseline for FST and corticosterone levels (Figure S11). We then placed aDTA mice under both T24 and T7 cycles and found no difference in anxiety-like behaviors between the two groups (Figure S12). In contrast, the increased depression-like behavior, learning deficits, and hippocampal LTP decrement observed in the T7 cycle in wild-type animals were not observed in aDTA mice exposed to this cycle (Figure 4). These results suggest that the negative influence of the aberrant light cycles on behavior requires ipRGCs. Thus, subconscious light detection in humans via ipRGCs may be responsible for the depression and learning deficits observed under disruptive light environments.

Manipulation of the light environment can lead to disruptions in circadian rhythms and sleep and also cause mood and learning defects in mice and humans^{2, 26, 27}. These studies have led to a model in which light affects cognition exclusively through the modulation of sleep and circadian pathways (Figure S13). Here, we provide an additional model whereby light directly influences mood leading to learning deficits in the context of an intact circadian timing system and normal sleep distribution and architecture (Figure S13A). Further support that the effects of the T7 cycle are not due to circadian disruptions originate from behavioral comparisons to animals lacking a functional circadian oscillator (e.g. circadian mutant- or SCN lesioned- animals), where in these animals, lower depression-like behavior is observed (Figure S13B)^{28, 29}. Taken together, these data provide evidence that the aberrant light effects on mood are direct. Furthermore, the depression-like behavior caused by the T7 aberrant light cycle can serve as an alternative experimental paradigm for depression research in rodents, independent of genetic manipulations or aversive treatments such as repetitive restraint or electric shocks.

Methods Summary

Animals and Housing

Adult (4–8 months) male mice (B6/129 F1 hybrid; Jackson Laboratory) were used for all experiments involving wild-type mice placed under different light environments. Adult littermates aDTA mice placed under different light environment were of B6/129 background (6–8 months) and were raised in our laboratory. aDTA mice could not be used until they were at least six months old because elimination of the melanopsin cell population in these mice is not complete until this time⁵. All mice were individually housed in standard animal facility cages with access to food and water ad libitum. All mice were initially entrained to a 12:12LD cycle (T24) after which the lights for one group were switched to 3.5:3.5LD (T7) for 2 weeks. The light intensity during the light portion was ~800lux, chosen to cause no circadian arrhythmicity. All experiments were done in accordance with the regulations set forth by Johns Hopkins University and Rider University Animal care and use committee.

Behavioral Analysis

Mice were maintained in the T24 or T7 light cycle for two weeks prior to testing unless otherwise indicated. Body temperature and general activity were measured to evaluate circadian rhythmicity. Sucrose preference and forced swim test were used to assess depression-like behavior. Morris Water Maze and Novel Object Recognition were used to assess hippocampal-dependent learning.

Cellular and Molecular Analysis

To examine the circadian timing system, immunohistochemistry and qRT-PCR were used to quantify *Per2* expression in the SCN and liver respectively. Serum corticosterone levels were quantified by ELISA. Electrophysiological recordings from the dorsal hippocampus were performed to evaluate hippocampal function including long-term potentiation and long-term depression.

Methods

Animals and Housing

Adult (4–8 months) male mice (B6/129 F1 hybrid; Jackson Laboratory) were used for all experiments involving wild-type mice placed under different light environments. Adult littermates aDTA mice placed under different light environment were of B6/129 background (6–8 months) and were raised in our laboratory. aDTA mice could not be used until they were at least six months old because elimination of the melanopsin cell population in these mice is not complete until this time⁵. All mice were individually housed in standard animal facility cages with access to food and water ad libitum. All mice were initially entrained to a 12:12LD cycle (T24) after which the lights for one group were switched to 3.5:3.5LD (T7) for 2 weeks. The light intensity during the light portion was ~800lux, chosen to have no circadian arrhythmicity. All experiments were done in accordance with the regulations set forth by Johns Hopkins University and Rider University Animal care and use committee.

Body Temperature Measurements

Body temperature measurements were made using G2 E-mitter telemetric probes from Mini mitter, Respironics (Bend, OR). The telemetric probe was implanted into the peritoneum and sutured to the inside of the abdominal wall. Mice were given 1 week to recover from surgery prior to any recording.

Recordings were obtained using Vitalview software (Respironics, Bend, OR), at a rate of 30 measurements/hour. Throughout experiment mice were maintained in their home cage without perturbation and the light cycles were adjusted to test response to both the T24 and T7 light cycles. Circadian period was determined by fitting a regression line to the onsets of activity over a 7-day period using Clocklab (Actimetrics, Wilmette, IL). Period lengths of mice housed in the T24 and T7 light cycles were compared using an unpaired student's t-test.

General Activity Measurements

General activity was measured using infrared motion detectors from Mini mitter, Respironics (Bend, OR). Mice were housed individually, and the motion detector was mounted to the top of the cage so that general activity could be monitored throughout the T24 and T7 light cycle. Data were collected in ten-minute bins using Vitalview software (Respironics, Bend, OR). Circadian period length was determined by fitting a regression line to the onsets of activity over a 7-day period using Clocklab (Actimetrics, Wilmette, IL). Period lengths of mice housed in the T24 and T7 light cycles were compared using an unpaired student's t-test.

Molecular Rhythm Measurements

Mice were housed in either the T24 (n=16) or T7 (n=16) light cycle for two weeks during which general activity was monitored in T7 mice to determine their circadian phase. Mice were sampled across four time points: Mice under the T24 cycle were sampled at ZT1, 7, 13, 19, and mice under the T7 cycle were sampled at CT1, 7, 13, 19 which was determined using their general activity rhythm. Each mouse was removed from its cage, and tail blood was quickly sampled. The mouse was then anesthetized with 1mL of Avertin (20mg/mL). Once anesthetized, a small sample of liver was isolated. The mouse was then perfused transcardially with 0.9% saline followed by 4% paraformaldehyde. The brain was removed and postfixed overnight in 4% paraformaldehyde followed by cryoprotection and embedding in OCT Compound (Sakura Finetek Torrance, CA).

Real-Time PCR: Liver samples were homogenized and RNA extracted using the RNeasy mini kit (Qiagen). The Retroscript kit (Ambion Austin, TX) was used to reverse transcribe poly(A) RNAs. Real-time qPCR was performed with iQ SYBR Green Supermix and the iCycler iQ real-time PCR detection system (Bio-Rad). Each sample was analyzed in triplicate reactions of 50 μ l. Primers for *Per2* were GCCTTCAGACTCATGATGACAGA and TTTGTGTGCGTCAGCTTTGG (reverse). Primers for 18S rRNA (internal control) were CGCCGCTAGAGGTGAAATTC (forward) and TTGGCAAATGCTTTTCGCTC (reverse). Data were analyzed using the $\Delta\Delta$ Ct method normalizing each sample to the internal control and relative mRNA was determined as the percentage of the maximum value observed in the experiment. Data were analyzed by two-way ANOVA followed by a Bonferroni post-hoc test to examine differences over time as well as potential light cycle effects on *Per2* expression.

PER2 Immunohistochemistry: Brains were sectioned (40 μ m) by cryostat through the rostral-caudal extent of the suprachiasmatic nucleus and were stored free floating in 0.1M phosphate buffer. Free floating sections were incubate in blocking buffer (0.1M phosphate buffer, 3% triton, 0.5% bovine serum albumin, 1% goat serum) for two hours. Sections were then incubated in rabbit anti-Per2 (Alpha Diagnostic International San Antonio, TX; 1:4000 in blocking buffer) overnight and visualized with a Vectastain horseradish peroxidase kit (Vector Labs Burlingame, CA) using DAB (Sigma St. Louis, MO). Sections were mounted on microscope slides, dehydrated, and coverslipped with Permount. Sections were imaged at 10 \times with a Zeiss Axio Imager M1 microscope. Optical density was measured using ImageJ.

Data were analyzed by two-way ANOVA followed by a Bonferroni post-hoc test to examine differences over time as well as potential light cycle effects on PER2 expression.

Corticosterone Measurement: Serum was isolated from collected tail blood and assayed for corticosterone by ELISA (Assaypro). Data were analyzed by two-way ANOVA followed by a Bonferroni post-hoc test to examine differences over time as well as light cycle effects on corticosterone levels. For fluoxetine experiments, corticosterone levels were analyzed by two-way ANOVA followed by a Bonferroni post-hoc to examine differences over time as well as the effect of fluoxetine.

For the experiment comparing WT and aDTA mice, serum was sampled from WT and aDTA mice at ZT13/CT13 based on general activity rhythms (as described above). The samples were processed as described above. Corticosterone levels of WT and aDTA mice were analyzed by unpaired student's t-test.

Light-Induced c-fos Expression

Mice were housed under a 12:12 LD cycle and were exposed to a 10-minute light pulse at ZT14 (two hours after light offset) after which they were placed back in the dark for 80 more minutes. Control mice remained in the dark until anesthetization. Ninety minutes after the start of light presentation, mice were deeply anesthetized with 1mL of Avertin (20mg/mL). Once anesthetized, the mice were perfused transcardially with 0.9% saline followed by 4% paraformaldehyde. Brains were removed, postfixed overnight in 4% paraformaldehyde, and then transferred to 0.1M phosphate buffer (PB). Brains were sectioned (40 μ m) through the rostro-caudal extent of the SCN using a vibrotome (World Precision Instruments). Sections were stored free-floating in 0.1M PB. Every other section was stained immunohistochemically for c-fos. Sections were incubated in blocking buffer (0.1M PB, 3% triton X-100, 0.5% bovine serum albumin (BSA)) for 2 hours. Sections were incubated in rabbit anti-c-fos (Calbiochem Ab-5; 1: 20,000) overnight at 4°C and then visualized with a goat anti-rabbit Vectastain horseradish peroxidase kit (Vector Labs, Burlingame, CA) using DAB (Sigma) as a chromagen. Sections were mounted on microscope slides, dehydrated, and coverslipped with Permount. Slides were viewed and imaged on a Zeiss Axio Imager.M1 microscope at 5 \times magnification. Photoshop and ImageJ were used to count c-fos positive cells and measure the area of region counted from. The number of c-fos positive cells was normalized to the area of the region, and these values were compared between mice that received a light pulse and dark controls. These data were analyzed using an unpaired student's t-test.

Sucrose Anhedonia

Mice were housed in the presence of two water bottles one day prior to testing to acclimate them to the bottles. Sucrose preference was assessed over two days. Each day, one bottle containing 1% sucrose and one bottle containing water were introduced at the beginning of the active phase. The position of these bottles was switched six hours later, and the bottles were removed at the end of the active phase. Bottles were weighed at the beginning and end of the active period to measure amount consumed. Sucrose preference was calculated by dividing the amount of sucrose consumed by the total amount consumed (water and sucrose). The percentage of sucrose consumed by mice in the T24 and T7 cycles was compared with a student's t-test.

Forced Swim Test

Mice were individually placed in an inescapable container of water (25°C) for 6 minutes. Behavior was monitored by video cameras positioned in front of the apparatus and scored by a video tracking system (Forced Swim Test, Bioserve). Time spent immobile for the last

four minutes of the test was calculated. Increased time spent immobile is indicative of increased depression-related behavior. The amount of time spent immobile during the last four minutes was analyzed by student's t-test. For fluoxetine experiments, the amount of time spent immobile during the last four minutes were analyzed by two-way ANOVA followed by a Bonferroni post-hoc to compare light cycle and drug treatment.

Open Field

Mice were individually placed in the center of a large, brightly lit arena (500lux, 60cm × 60cm) and allowed to explore for five minutes. Behavior was monitored from above by a video camera connected to a computerized video tracking system (Anymaze, Stoelting). The apparatus was cleaned thoroughly between each trial. Percent distance traveled and time in the center of the arena were measured. These measures were compared between mice housed in the T24 and T7 mice using an unpaired student's t-test.

Light Dark Box

The light dark box consisted of two compartments equivalent in size (20cm × 20cm); one area is brightly lit (600lux) and the other is dimly lit (<1lux). A small opening joins the two compartments, so the mice could freely move between the two areas. Mice were dark adapted for one hour prior to testing. At the beginning of the test, dark-adapted mice were placed in the lit compartment facing away from the opening and allowed to freely explore for five minutes. Behavior was monitored from above by a video camera connected to a computerized video tracking system (Anymaze, Stoelting). The apparatus was cleaned thoroughly between each trial. The number of transitions between the two compartments as well as the time spent and distance travelled in the lit room were measured as indications of anxiety-related behavior. These measures were compared between mice housed in the T24 and T7 mice using an unpaired student's t-test.

Elevated Plus Maze

The apparatus consisted of two open arms (42cm × 6cm) opposite to one another and two arms enclosed by walls (42cm × 6cm × 14cm) opposite of one another forming a cross. The arms were separated by a central platform (6cm × 6cm). The maze was elevated (33cm) such that the open arms convey openness, unfamiliarity, and elevation. The light intensity in the open arms was ~600 lux while the light intensity in the closed arms was ~ 200lux. Mice were placed in the center of the elevated plus maze facing one of the open arms. Behavior was monitored from above by a video camera connected to a computerized video tracking system (Anymaze, Stoelting). The apparatus was cleaned thoroughly between each trial. The time spent and distance travelled in the open arms were measured as indications of anxiety-related behavior. These measures were compared between mice housed in the T24 and T7 mice using an unpaired student's t-test.

Morris Water Maze

The water maze consisted of a circular pool (150 cm in diameter) with room temperature water (26–28°C). The water was made opaque with the addition of non-toxic white tempura paint to hide the escape platform. The platform was made from PVC piping with a top (10 cm in diameter) painted white and submerged in the pool such that (1 cm) of water covered the platform hiding it from sight. For visual trials, a flag made from a 50 ml conical tube covered with colored tape was placed on the platform. During the acquisition, probe and reversal trials, four cues were attached to the side of the pool equidistant from one another, and the entire pool was surrounded by a plain curtain to block any other visual cues. Performance was scored using a video tracking system (Anymaze, Stoelting) with a camera mounted above the pool. The light intensity at the water surface was approximately 500lux.

Mice were tested in four stages: visual, acquisition, probe, and reversal (see Figure 2A). Before spatial training, mice were trained to escape the pool using the visual flag located on top of the platform to familiarize them with the test. This was performed four times with an inter-trial interval of (30 minutes), and the platform was moved between each trial. We also used this visual training to screen for and remove animals that show floating behavior in the water maze. Animals that floated in two or more trials during training were not tested in the spatial task to prevent confounds from floating behavior. During the acquisition phase, mice were trained (one trial per day for twelve days) to find the hidden platform using the four visual distal cues surrounding the pool. The mouse was randomly placed in a different area of the pool at the start of each trial with the platform maintained in the same quadrant (target quadrant). The platform was removed on Day 13 in the probe trial. The swimming in each quadrant and specifically the preference for the target quadrant was measured to evaluate spatial memory using a computerized video tracking system (Anymaze, Stoelting). Reversal training began on Day 14 where the platform was moved to the quadrant opposite the original target quadrant. Mice were trained as described for the acquisition phase.

Latency to locate the platform during the acquisition and reversal phases was analyzed by two-way ANOVA followed by a Bonferroni post-hoc test to examine changes in latency throughout the course of the experiment as well as the effect of light cycle exposure. Probe Trial was analyzed by calculating the percent time spent in the target quadrant and performing a one sample t-test to determine if this was significantly above 25%.

Novel Object Recognition

NOR was composed of three stages: acclimation to the novel object arena, familiar object exposure, and finally novel object exposure. Mice were first removed from their home cage, acclimated to the empty testing arena (light intensity of 500lux) for 10 minutes, and subsequently returned to their home cage 24-hours before including two objects in the arena. The day after acclimation, mice were returned to this arena with two identical objects that they could freely explore for 10 minutes, after which they were returned to their home cage for one hour. At the end of the 1-hour period, mice were placed back into the arena with one of the objects changed to a novel object and allowed to explore both the familiar and novel objects for 5 minutes. Behavior was monitored from above by a video camera connected to a computerized video tracking system (Anymaze, Stoelting), and the percentage of time spent with each object was calculated. Wild-type mice spend more time with the novel object, however mice with recognition memory deficits will not be able to distinguish the novel from the stable object. Objects had been previously tested to ensure that animals showed no initial preference for a particular object. Identity of the objects (familiar versus novel) was counterbalanced. The objects and arena were thoroughly cleaned between each trial to remove odor cues. Object recognition was analyzed by calculating the percent time spent with the novel object and performing a one sample t-test to determine if this was significantly above 50%.

Slice Electrophysiology

Coronal (0.4 mm) hippocampal slices were prepared as described³⁰ in ice-cold dissection buffer (2.6 mM KCl, 1.23mM NaH₂PO₄, 26mM NaHCO₃, 212.7 mM sucrose, 10mM dextrose, 3mM MgCl₂, and 1mM CaCl₂ bubbled with 5% CO₂/95% O₂). Recordings were done in a similar buffer but with the sucrose replaced by NaCl and the temperature raised to 30 degrees. Synaptic responses were evoked at 0.33 Hz stimulating the Schaffer collaterals with 0.2 ms pulses (concentric bipolar electrodes FHC), and recorded extracellularly in CA1 stratum radiatum. Long-Term Potentiation (LTP) was induced by theta burst stimulation (TBS), consisting of one or four theta epochs delivered at 0.1 Hz. Each epoch, in turn, consisted of 10 trains of four pulses (at 100 Hz) delivered at 5 Hz. Long-Term Depression

(LTD) was induced by low frequency stimulation (1 Hz, 15 min). These protocols were delivered following 20 min of stable baseline transmission. All hippocampal slice electrophysiological recordings were performed and analyzed by an experimenter blind to the treatment of the animals. Two-way ANOVA was used to analyze fiber volley differences between the T7 and T24 treatments. The slopes for the linear fit of the FV-Slope relationship were compared by t-test.

Fluoxetine Administration

Mice were housed in either the T24 or T7 cycle for two weeks (n=20 per group) with food and water ad libitum. For chronic treatment, this was followed by a three-week treatment of 18mg/kg/day of fluoxetine (Sigma). For subchronic treatment, this was followed by a four-day treatment of 18mg/kg/day. Fluoxetine was administered in the drinking water and control mice received tap water. Dosage was calculated based on the average amount of water consumed per day and mouse weight. Fluoxetine consumption was also measured during treatment to determine the amount consumed per mouse.

Period Length Measurement with Fluoxetine Treatment

Mice were housed under infrared motion detectors as described above. Mice were housed in the T7 light cycle for two weeks after which fluoxetine (18mg/kg/day) was administered in the drinking water for three weeks. Circadian period was determined by fitting a regression line to the onsets of activity over a 7-day period. Period lengths before and after three weeks of fluoxetine treatment were compared by paired t-test.

Desipramine Administration

Desipramine (Sigma) was dissolved in sterile water with 5% Tween-20. Each mouse received 16 mg/kg desipramine (i.p.) 24- and 1-hour prior to testing in the novel object recognition paradigm. The same volume of vehicle (water with 5% Tween-20) was administered (i.p.) to control mice.

Statistical Analysis

All statistical analysis was performed using GraphPad Prism. Specific tests used to analyze data are described their respective section of the methods.

Supplementary Material

Refer to Web version on PubMed Central for supplementary material.

Acknowledgments

We would like to thank Drs. Todd Gould, Gregory Ball and Akira Sawa for their expert advice on the behavioral tests. We would like to thank Dr. Rejji Kuruvilla for her critical reading and advice on this manuscript. We would also like to thank the mouse tri-lab for suggestions and advice. This work was supported by the David and Lucile Packard Foundation grant to SH.

References

1. Reppert SM, Weaver DR. Coordination of circadian timing in mammals. *Nature*. 2002; 418:935–41. [PubMed: 12198538]
2. Foster RG, Wulff K. The rhythm of rest and excess. *Nat Rev Neurosci*. 2005; 6:407–14. [PubMed: 15861183]
3. Berson DM, Dunn FA, Takao M. Phototransduction by retinal ganglion cells that set the circadian clock. *Science*. 2002; 295:1070–3. [PubMed: 11834835]

4. Hattar S, Liao HW, Takao M, Berson DM, Yau KW. Melanopsin-containing retinal ganglion cells: architecture, projections, and intrinsic photosensitivity. *Science*. 2002; 295:1065–70. [PubMed: 11834834]
5. Guler AD, et al. Melanopsin cells are the principal conduits for rod-cone input to non-image-forming vision. *Nature*. 2008; 453:102–5. [PubMed: 18432195]
6. Hattar S, et al. Central projections of melanopsin-expressing retinal ganglion cells in the mouse. *J Comp Neurol*. 2006; 497:326–49. [PubMed: 16736474]
7. Klerman EB, et al. Photic resetting of the human circadian pacemaker in the absence of conscious vision. *J Biol Rhythms*. 2002; 17:548–55. [PubMed: 12465888]
8. Zaidi FH, et al. Short-wavelength light sensitivity of circadian, pupillary, and visual awareness in humans lacking an outer retina. *Curr Biol*. 2007; 17:2122–8. [PubMed: 18082405]
9. Altimus CM, et al. Rods-cones and melanopsin detect light and dark to modulate sleep independent of image formation. *Proc Natl Acad Sci U S A*. 2008; 105:19998–20003. [PubMed: 19060203]
10. Lam RW, Levitan RD. Pathophysiology of seasonal affective disorder: a review. *J Psychiatry Neurosci*. 2000; 25:469–80. [PubMed: 11109298]
11. Nestler EJ, et al. Neurobiology of depression. *Neuron*. 2002; 34:13–25. [PubMed: 11931738]
12. McEwen BS. Protective and damaging effects of stress mediators. *N Engl J Med*. 1998; 338:171–9. [PubMed: 9428819]
13. Cryan JF, Holmes A. The ascent of mouse: advances in modelling human depression and anxiety. *Nat Rev Drug Discov*. 2005; 4:775–90. [PubMed: 16138108]
14. Baldi E, Lorenzini CA, Corrado B. Task solving by procedural strategies in the Morris water maze. *Physiol Behav*. 2003; 78:785–93. [PubMed: 12782236]
15. Vorhees CV, Williams MT. Morris water maze: procedures for assessing spatial and related forms of learning and memory. *Nat Protoc*. 2006; 1:848–58. [PubMed: 17406317]
16. Bliss TV, Collingridge GL. A synaptic model of memory: long-term potentiation in the hippocampus. *Nature*. 1993; 361:31–9. [PubMed: 8421494]
17. McDermott CM, et al. Sleep deprivation causes behavioral, synaptic, and membrane excitability alterations in hippocampal neurons. *J Neurosci*. 2003; 23:9687–95. [PubMed: 14573548]
18. Honey RC, Watt A, Good M. Hippocampal lesions disrupt an associative mismatch process. *J Neurosci*. 1998; 18:2226–30. [PubMed: 9482806]
19. Valentinuzzi VS, Menna-Barreto L, Xavier GF. Effect of circadian phase on performance of rats in the Morris water maze task. *J Biol Rhythms*. 2004; 19:312–24. [PubMed: 15245650]
20. Dulawa SC, Holick KA, Gundersen B, Hen R. Effects of chronic fluoxetine in animal models of anxiety and depression. *Neuropsychopharmacology*. 2004; 29:1321–30. [PubMed: 15085085]
21. Sprouse J, Braselton J, Reynolds L. Fluoxetine modulates the circadian biological clock via phase advances of suprachiasmatic nucleus neuronal firing. *Biol Psychiatry*. 2006; 60:896–9. [PubMed: 16631132]
22. Lockley SW, et al. Short-wavelength sensitivity for the direct effects of light on alertness, vigilance, and the waking electroencephalogram in humans. *Sleep*. 2006; 29:161–8. [PubMed: 16494083]
23. Vandewalle G, et al. Spectral quality of light modulates emotional brain responses in humans. *Proc Natl Acad Sci U S A*. 2010; 107:19549–54. [PubMed: 20974959]
24. Iyilikci O, Aydin E, Canbeyli R. Blue but not red light stimulation in the dark has antidepressant effect in behavioral despair. *Behav Brain Res*. 2009; 203:65–8. [PubMed: 19379775]
25. Warthen DM, Wiltgen BJ, Provencio I. Light enhances learned fear. *Proc Natl Acad Sci U S A*. 2011; 108:13788–93. [PubMed: 21808002]
26. Fonken LK, et al. Influence of light at night on murine anxiety- and depressive-like responses. *Behav Brain Res*. 2009; 205:349–54. [PubMed: 19591880]
27. Ma WP, et al. Exposure to chronic constant light impairs spatial memory and influences long-term depression in rats. *Neurosci Res*. 2007; 59:224–30. [PubMed: 17692419]
28. Roybal K, et al. Mania-like behavior induced by disruption of CLOCK. *Proc Natl Acad Sci U S A*. 2007; 104:6406–11. [PubMed: 17379666]

29. Tataroglu O, Aksoy A, Yilmaz A, Canbeyli R. Effect of lesioning the suprachiasmatic nuclei on behavioral despair in rats. *Brain Res.* 2004; 1001:118–24. [PubMed: 14972660]
30. Lee HK, Min SS, Gallagher M, Kirkwood A. NMDA receptor-independent long-term depression correlates with successful aging in rats. *Nat Neurosci.* 2005; 8:1657–9. [PubMed: 16286930]

\$watermark-text

\$watermark-text

\$watermark-text

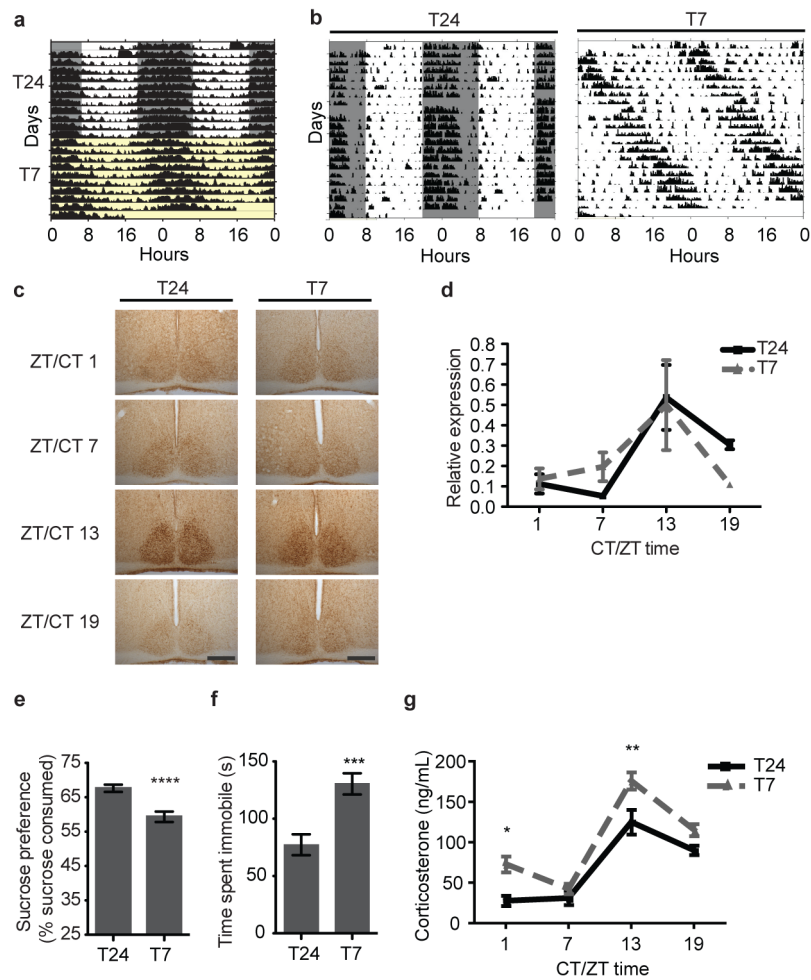


Figure 1. Aberrant light increases depression-like behavior and corticosterone levels
A. Body temperature rhythms under the T24 (grey/white) and T7 (yellow) cycle. **B.** General activity rhythms under the T24 (left) and T7 cycle (right). **C.** SCN PER2 was rhythmic under the T24 and T7 cycles. Scale bars, 200 μ m. **D.** Liver *Per2* was rhythmic ($p_{\text{time}}=0.0072$) ($n=3-4$ per time point, $p_{\text{light cycle}}=0.8482$). **E.** T7 mice showed sucrose anhedonia ($n=16,15$, $p<0.0001$). **F.** T7 mice showed increased immobility in the FST ($n=22$ per group, $p=0.0002$). **G.** Corticosterone levels were rhythmic but elevated in T7 mice ($n=5-6$ per timepoint, $p_{\text{time}}<0.0001$, $p_{\text{light cycle}}<0.0001$, Bonferroni post-test: $p<0.05$ ZT/CT 1 and $p<0.01$ ZT/CT13). **** $p<0.0001$, *** $p<0.001$, ** $p<0.01$, * $p<0.05$. Error bar indicates SEM.

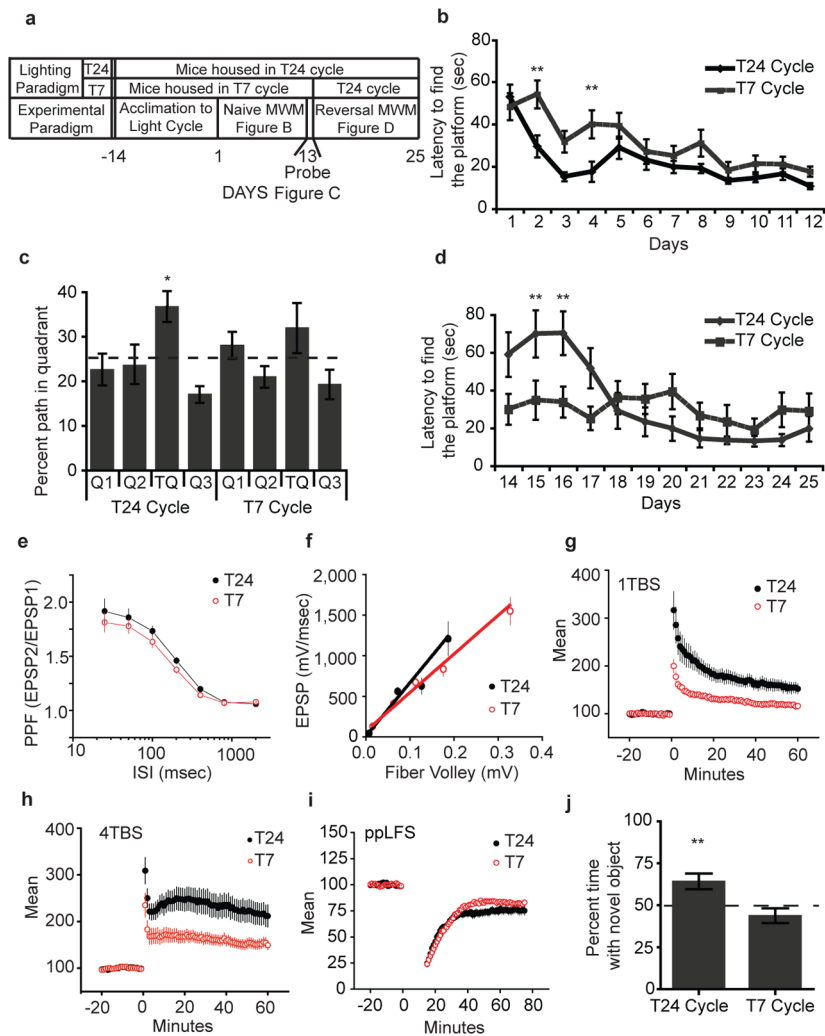


Figure 2. Aberrant light impairs hippocampal learning, LTP, and recognition memory
A. Experimental paradigm for the MWM. **B.** T7 mice showed impaired learning ($n=21$ per group, $p_{\text{interaction}}=0.041$, Bonferroni post-test $p<0.01$ days 2 and 4). **C.** T7 mice show no significant preference for the target quadrant (T24: $n=9$, $p=0.011$; T7: $n=9$, $p=0.25$). Dotted line indicates chance (25%). **D.** Mice housed in the T24 cycle showed an increased latency in a reversal trial, whereas, T7 housed mice show a similar latency to the acquisition phase ($n=9$ per group, $p_{\text{interaction}}<0.0003$, Bonferroni post-test $p<0.01$ days 15 and 16). **E and F.** T24 and T7 mice have similar basal synaptic release properties ($p_{\text{interaction}}=0.7256$) ($n=5$ per group) (Fiber volley: $p_{\text{interaction}}=0.984$, Slope: $p>0.1$). **G–I.** T7 mice showed LTP deficits ($n=5$ per group, 1 TBS: $p_{\text{interaction}}<0.01$; 4 TBS: $p_{\text{interaction}}<0.01$) (G and H) but no difference in LTD (I). **J.** T7 mice showed deficit in novel object recognition (T24: $n=24$, $p=0.0057$; T7: $n=24$, $p=0.1773$). * $p<0.05$. Error bar indicates SEM.

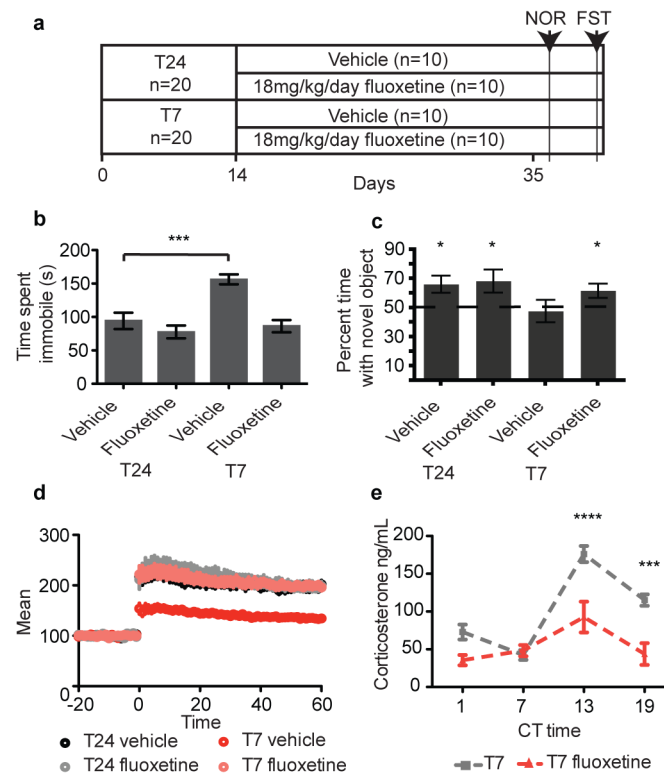


Figure 3. Chronic antidepressant administration rescues learning

A. Timeline for fluoxetine administration and testing **B.** Chronic fluoxetine reduced T7 immobility time in the FST ($n=10$ per group, $p_{\text{interaction}}=0.0092$, Bonferroni posttest $p<0.001$ T24 vs T7 vehicle) **C.** T7 mice treated with fluoxetine showed restored novel object preference (T24_{vehicle}: $n=9$, $p=0.03$; T24_{fluoxetine}: $n=9$, $p=0.048$; T7_{vehicle}: $n=10$, $p=0.77$; T7_{fluoxetine}: $n=10$, $p=0.04$). **D.** Chronic fluoxetine rescued the T7-induced LTP deficit ($n=5,4$; $p_{\text{interaction}}<0.0001$). **E.** Chronic fluoxetine decreased corticosterone levels in T7 mice ($n=5-8$ per time point). T7 corticosterone levels are plotted for comparison. ($p_{\text{interaction}}=0.0053$, Bonferroni post-test $p<0.0001$ CT13 and $p<0.001$ CT19) **** $p<0.0001$, *** $p<0.001$, * $p<0.05$. Error bar indicates SEM.

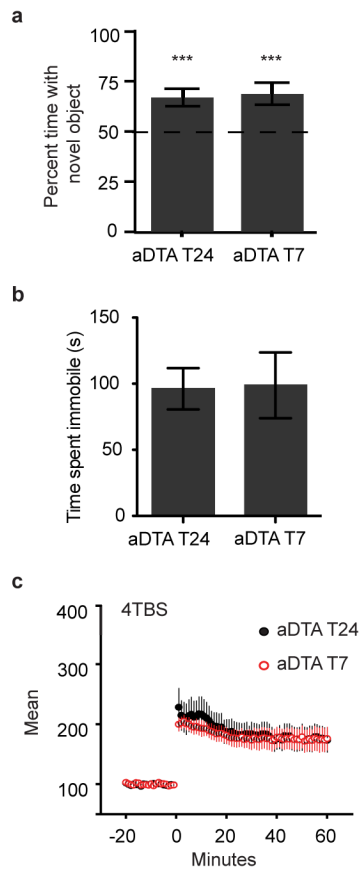


Figure 4. ipRGCs mediate impairment of mood and learning by aberrant light

A. Mice lacking ipRGCs showed a significant preference for the novel object when housed both in the T24 and T7 light cycles (n=12 per group, $p < 0.001$). **B.** aDTA mice housed in the T7 cycle performed similarly to aDTA mice housed in the T24 cycle in the FST (n=6,5, unpaired t-test $p = 0.93$). **C.** T7 aDTA mice had LTP similar to T24 aDTA mice in response to 4-pulse theta burst stimulation. *** $p < 0.001$. Error bar indicates SEM.